

A NEW DEFORMED POTENTIAL IN EXPLAINING  
THE  $\alpha$ -DECAY\*AYDIN YILDIRIM<sup>a,†</sup>, DILSHOD ALIMOV<sup>b,c,‡</sup>, MARDAN BAKIROV<sup>b,§</sup>  
YASEMIN KUCUK<sup>a,¶</sup>, İSMAIL BOZTOSUN<sup>a,||</sup><sup>a</sup>Department of Physics, Akdeniz University, Antalya, Turkey<sup>b</sup>Institute of Nuclear Physics, 050032 Ibragimova 1, Almaty, Kazakhstan<sup>c</sup>Al-Farabi Kazakh National University

050040 Al-Farabi, 71, Almaty, Kazakhstan

*Received 14 November 2022, accepted 16 November 2022,**published online 26 January 2023*

In this paper, we investigate the role of potential deformation in explaining the  $\alpha$ -decay. The deformation of the nuclear potential has been taken into account by adding a Gaussian potential to the well-known Wood-Saxon potential. For the numerical calculations, the Wentzel-Kramers-Brillouin method has been used, and also the Bohr-Sommerfeld quantization condition has been employed to restrict the parameters. The half-lives of ten nuclei have been calculated for  $\alpha$ -decay and very good agreement has been obtained with the experimental data.

DOI:10.5506/APhysPolBSupp.16.2-A1

## 1. Introduction

The  $\alpha$ -decay is the direct result of the quantum tunneling process through the Coulomb barrier and it is shown by Gamow [1] and Gurney and Condon [2] separately. The work of Gamow led him to derive analytical solutions to get the half-lives of the interested parent nuclei. Geiger and Nuttall [3] studied the same phenomena experimentally. The works of these scientists lead to the developed cluster models in nuclear physics [4–8]. The cluster models have a very important role in nuclear physics for two basic reasons. Firstly, they may be used for a better understanding of the existing nuclei and secondly, they may lead scientists to create new super-heavy nuclei

---

\* Presented at the IV International Scientific Forum *Nuclear Science and Technologies*, Almaty, Kazakhstan, 26–30 September, 2022.

<sup>†</sup> aydinyldrm@gmail.com

<sup>‡</sup> d\_alimov@inp.kz

<sup>§</sup> b.mardan@mail.ru

<sup>¶</sup> ykucuk@akdeniz.edu.tr

<sup>||</sup> boztosun@akdeniz.edu.tr

in particle accelerators [9–12]. Thus, in order to better understand cluster models, studying the  $\alpha$ -decay mechanism has a critical role. The mechanism of  $\alpha$ -decay is a widely studied topic. In order to understand the  $\alpha$ -decay, realistic nuclear potentials are proposed in many studies and the experimental data were compared [4–21].

In order to study  $\alpha$ -decay, one needs to solve the Schrödinger equation. There are many attempts to solve the Schrödinger equation with a suitable potential, however, only a few of them have analytical solutions. The rest require numerical methods to get a solution [22–24]. Although there are numerous successful potentials, they are not suitable for all the nuclei or they do not completely explain the nuclear structure. Especially, the deformation of the surface region creates problems for these nuclear potentials. In order to overcome these effects, more realistic potentials are required. Considering these problems, we have proposed a new realistic nuclear potential. Simply, we have taken the Wood–Saxon potential and added a second term to disturb the surface region. We have used the Gaussian potential as a perturbation term. We have used the Wentzel–Kramers–Brillouin (WKB) method in our calculations along with the Bohr–Sommerfeld quantization conditions. We should point out that the shape of the nuclear potential directly affects the WKB approach [25].

This study has been organized as follows: in the following section, we introduce the theoretical model. Then, we present the results comparing with the experimental data. Finally, we present the conclusion of this work.

## 2. Model

In a realistic nuclear model, there are three parts that shape the potential: the Coulomb, centrifugal, and nuclear potential. The sum of these three potentials is called effective potential. For the  $\alpha$ -decay, the shape of the effective potential, especially the shape of the surface is important [26–29]. Equation (1) defines the effective potential with radial distance  $r$

$$V_{\text{eff}}(r) = V_C(r, \theta) + V_L(r) + V_N(r, \theta). \quad (1)$$

The Coulomb potential and centrifugal potential are well known. However, the nuclear potential is still a hot topic and there are numerous suggested models. One of the well-known potentials is the Wood–Saxon potential. Although it is a successful model, it is not very successful for the agreement with all the nuclei. Therefore, we suggest a new methodology where we add a Gaussian term to the Wood–Saxon potential in order to take into account a deformation effect. The model used in our calculation is given as follows:

$$V_N(r, \theta) = -\lambda(\theta) \frac{V_0}{1 + e^{\frac{r-R}{a}}} + V_1 e^{[-(r-R)^2]}. \quad (2)$$

Here,  $R = r_0 A_d^{1/3}$  is the nuclear radius and  $A_d^{1/3}$  is the atomic mass of the daughter nucleus.  $\lambda(\theta)$  is the normalization parameter and it comes from the restriction of the Bohr–Sommerfeld quantization condition.  $a$  is the diffusion parameter,  $V_0$  and  $V_1$  are the depth of the nuclear potential. Finally,  $\theta$  is the orientation angle. As can be seen in equation (2), the first part is the well-known Wood–Saxon potential and the second part is a Gaussian term. The role of the Gaussian part is to deform the surface. Figure 1 shows the difference between the Wood–Saxon potential and the suggested potential. In figure 1, one can see the deformation in the surface region compared to the Wood–Saxon potential.

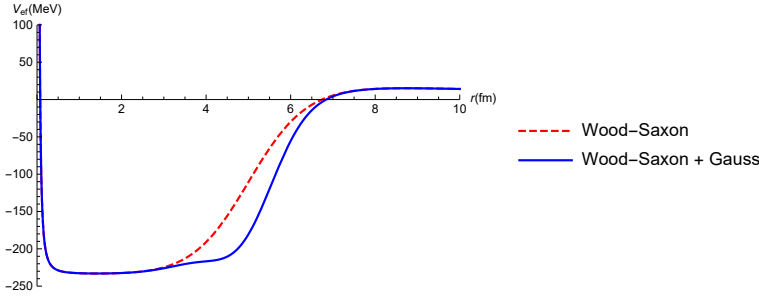


Fig. 1. (Color online) The dashed red line shows the shape of the effective potential for Wood–Saxon. The blue line shows the shape of the proposed effective potential namely Wood–Saxon+Gauss.

The Coulomb potential is a well known potential and may be given as

$$V_C(r) = \begin{cases} \frac{Z_\alpha Z_d e^2}{r}, & r \geq R, \\ \frac{Z_\alpha Z_d e^2}{2R} \left[ 3 - \left( \frac{r}{R} \right)^2 \right], & r < R. \end{cases} \quad (3)$$

In equation (3),  $Z_d$  and  $Z_\alpha$  are the charges of the daughter nucleus and the  $\alpha$  particle, respectively. This potential can be written in two parts: the inner part and the outer part of the nuclear radius. Since the charge of the  $\alpha$  particle has a uniform shape and the daughter nucleus has not, there is a discontinuity at  $r = R$ . In order to overcome this discontinuity, the Coulomb potential may be re-written in the form of equations (4) and (5) [30, 31] as

$$\tilde{V}_C(r, \theta) = \frac{Z_\alpha Z_d e^2}{r} \left[ 1 - e^{-\varphi(\theta)r - \frac{1}{2}(\varphi(\theta)r)^2 - 0.35(\varphi(\theta)r)^3} \right], \quad (4)$$

$$\varphi = \frac{1}{R} \frac{3}{2}. \quad (5)$$

The centrifugal potential is also a well-known potential and by using Langer modifications, it can be written as [32]

$$V_L(r) = \frac{\hbar^2 \left(L + \frac{1}{2}\right)^2}{2\mu r^2}. \quad (6)$$

In this notation,  $\mu$  is the reduced mass of the daughter nucleus and  $\alpha$  particle, while the  $L$  shows the angular momentum. The half-life of a nucleus can be calculated using the equation [5, 6, 33]

$$T_{1/2} = \hbar \frac{\ln 2}{\Gamma}. \quad (7)$$

In equation (7),  $\Gamma$  represents the  $\alpha$ -decay width. In semi-classical theory, the  $\Gamma$  value for each of the nuclei can be found as [6]

$$\Gamma = P\bar{F} \frac{\hbar^2}{4\mu} \bar{S}. \quad (8)$$

In equation (8), there are three parameters that have to be fixed. The first parameter is  $P$  which is the pre-formation factor, the second parameter is the average of the normalization factor and it is represented by  $\bar{F}$ , and finally,  $\bar{S}$  is the average of the transition probability. The pre-formation factor can be found as [34–36]

$$P_\alpha = \begin{cases} 1.0, & \text{even-even nuclei,} \\ 0.6, & \text{odd-}A \text{ nuclei,} \\ 0.35, & \text{odd-odd nuclei.} \end{cases} \quad (9)$$

The analytical calculations are very difficult to solve for calculating the half-lives but the numerical solutions may provide reasonable results. In the previous studies of Coban *et al.* [31] and Yıldırım *et al.* [21], these numerical solutions have yielded very good results. In the following sections, we present our results obtained by deformed nuclear potential with a comparison of the experimental data.

### 3. Results and discussion

The half-lives of ten unstable nuclei have been calculated in this study. In order to calculate the half-lives, we have employed the Wentzel–Kramers–Brillouin method and we have also used the Bohr–Sommerfeld quantization conditions to restrict equations. These ten nuclei have been chosen between the atomic mass numbers of  $A = 106$  and  $A = 198$ .

The results of the numerical half-life calculations are given in Table 1. The first column of Table 1 is the nuclei which we have chosen. The next column shows the  $Q$  values of the  $\alpha$ -decay of each nuclei. In the third column, there are given the experimentally measured half-lives of these nuclei. The next column shows the numerically calculated half-lives of this study and they are labeled  $T^{\text{Gauss}}_{1/2}$  in order to show the effect of the deformation by adding the Gauss potential. The last column shows the deviation of the experimental and calculated half-lives for each of the chosen nuclei in the decimal logarithm.

Table 1. The comparison between experimental data and numerically produced data. The  $Q$  values and deviations of experimental and calculated data are also presented in the table.

Nuclei	$Q_{\alpha}$ [MeV]	$T^{\text{exp}}_{1/2}$	$T^{\text{Gauss}}_{1/2}$	$\log_{10} \frac{T^{\text{exp}}_{1/2}}{T^{\text{theo}}_{1/2}}$
$^{106}\text{Te} \rightarrow ^{102}\text{Sn} + \alpha$	4.290	60 $\mu\text{s}$	73.9 $\mu\text{s}$	-0.090
$^{107}\text{Te} \rightarrow ^{103}\text{Sn} + \alpha$	4.008	3.1 ms	2.72 ms	0.056
$^{108}\text{Te} \rightarrow ^{104}\text{Sn} + \alpha$	3.445	2.1 s	2.6 s	-0.092
$^{144}\text{Nd} \rightarrow ^{140}\text{Ce} + \alpha$	1.905	$2.29 \times 10^{15}$ y	$6.52 \times 10^{15}$ y	-0.454
$^{152}\text{Er} \rightarrow ^{148}\text{Dy} + \alpha$	4.934	10.3 s	12.4 s	-0.082
$^{153}\text{Er} \rightarrow ^{149}\text{Dy} + \alpha$	4.802	37.1 s	62.6 s	-0.227
$^{153}\text{Tm} \rightarrow ^{149}\text{Ho} + \alpha$	5.248	1.48 s	2.24 s	-0.180
$^{196}\text{At} \rightarrow ^{192}\text{Bi} + \alpha$	7.198	387 ms	457 ms	-0.073
$^{198}\text{At} \rightarrow ^{194}\text{Bi} + \alpha$	6.889	1.25 s	5.56 s	-0.096
$^{198}\text{Rn} \rightarrow ^{194}\text{Po} + \alpha$	7.349	65 ms	121 ms	-0.272

As seen in Table 1, the experimental half-lives and the new calculated half-lives are in very good agreement with each other. Clearly, this deformed potential is promising for the calculation of the half-lives of the unstable nuclei in the sense of  $\alpha$ -decay.

#### 4. Conclusion

In this paper, we have investigated the half-lives of ten unstable nuclei for the  $\alpha$ -decay. We have used the standard Wood–Saxon nuclear potential with a Gaussian term to take into account the surface deformation. We have also calculated the half-lives of the chosen nuclei numerically by employing the Wentzel–Kramers–Brillouin method and also using the Bohr–Sommerfeld quantization conditions. The new deformed nuclear potential provides very good explanations to the experimental data and further applications of this new potential will be performed for medium, heavy, and super-heavy nuclei.

## REFERENCES

- [1] G. Gamow, *Z. Phys.* **51**, 204 (1928).
- [2] R.W. Gurney, E.U. Condon, *Nature* **122**, 439 (1928).
- [3] H. Geiger, J.M. Nuttall, *Philos. Mag.* **22**, 613 (1911).
- [4] B. Buck, J.C. Johnston, A.C. Merchant, S.M. Perez, *Phys. Rev. C* **52**, 1840 (1995).
- [5] B. Buck, A.C. Merchant, S.M. Perez, *Phys. Rev. Lett.* **76**, 380 (1996).
- [6] C. Xu, Z. Ren, *Phys. Rev. C* **74**, 014304 (2006).
- [7] A. Soylu, Y. Sert, O. Bayrak, I. Boztosun, *Eur. Phys. J. A* **48**, 128 (2012).
- [8] A. Soylu, O. Bayrak, *Eur. Phys. J. A* **51**, 46 (2015).
- [9] S. Hofmann *et al.*, *Eur. Phys. J. A* **10**, 5 (2001).
- [10] Yu.Ts. Oganessian *et al.*, *Phys. Rev. C* **74**, 044602 (2006).
- [11] Yu.Ts. Oganessian, V.K. Utyonkov, *Nucl. Phys. A* **944**, 62 (2015).
- [12] Yu.Ts. Oganessian, V.K. Utyonkov, *Rep. Prog. Phys.* **78**, 036301 (2015).
- [13] H. Koura, *J. Nucl. Sci. Tech.* **49**, 816 (2012).
- [14] F. Koyuncu, A. Soylu, O. Bayrak, *Mod. Phys. Lett. A* **32**, 1750050 (2017).
- [15] B.R. Sivasankaran, M.A. Christas, K.V. Aarthi, M.J. Larny, *Nucl. Phys. A* **989**, 246 (2019).
- [16] M.R. Pahlavani, S. Rahimi Shamami, *Chinese J. Phys.* **66**, 733 (2020).
- [17] O. Bayrak, *J. Phys. G: Nucl. Part. Phys.* **47**, 025102 (2020).
- [18] J. Zhang, H.F. Zhang, *Phys. Rev. C* **102**, 044308 (2020).
- [19] F. Ghorbani, S.A. Alavi, V. Dehghani, *Nucl. Phys. A* **1006**, 122111 (2021).
- [20] P. Jachimowicz, M. Kowal, J. Skalski, *At. Data Nucl. Data Tables* **138**, 101393 (2021).
- [21] A. Yildirim, İ. Boztosun, D. Kaya, Y. Küçük, *Braz. J. Phys.* **52**, 40 (2022).
- [22] M. Aygun, O. Bayrak, I. Boztosun, Y. Sahin, *Eur. Phys. J. D* **66**, 35 (2012).
- [23] O. Bayrak, İ. Boztosun, *Int. J. Quantum Chem.* **107**, 1040 (2007).
- [24] I. Boztosun, W.D.M. Rae, *Phys. Lett. B* **518**, 229 (2001).
- [25] J. Dong, W. Zuo, W. Scheid, *Nucl. Phys. A* **861**, 1 (2011).
- [26] G. Igo, *Phys. Rev. Lett.* **1**, 72 (1958).
- [27] G. Igo, *Phys. Rev.* **115**, 1665 (1959).
- [28] J. Cook, J.M. Barnwell, N.M. Clarke, R.J. Griffiths, *J. Phys. G: Nucl. Phys.* **6**, 1251 (1980).
- [29] T. Vertse, K.F. Pál, Z. Balogh, *Comput. Phys. Commun.* **27**, 309 (1982).
- [30] D.M. Brink, N. Takigawa, *Nucl. Phys. A* **279**, 159 (1977).
- [31] A. Coban, O. Bayrak, A. Soylu, I. Boztosun, *Phys. Rev. C* **85**, 044324 (2012).
- [32] R.E. Langer, *Phys. Rev.* **51**, 669 (1937).
- [33] V.Y. Denisov, A.A. Khudenko, *At. Data Nucl. Data Tables* **95**, 815 (2009).
- [34] C. Xu, Z. Ren, *Nucl. Phys. A* **753**, 174 (2005).
- [35] C. Xu, Z. Ren, *Nucl. Phys. A* **760**, 303 (2005).
- [36] P.E. Hodgson, E. Běták, *Phys. Rep.* **374**, 1 (2003).